

## The Mathematical Description of End Mill Cutters and Effective Radius of Tool Geometry on Multi-Axis Milling

Dr. Ahmed A. Abdulwahhab\*, Dr. Jamal H. Mohamed\*  
& Dr. Bahha I. Kazem\*\*

Received on: 26/5/2009

Accepted on: 7/1/2010

### Abstract

The mathematical modeling and detailed algorithms are derived in this paper to describe the geometrical shape of end mill cutters for multi-axis milling machining. Details of the geometry analysis techniques are presented to understand the effective cutting shape. Three types of cutters are taken in the present paper. Finally, the procedures of finding the instantaneous cutting profile and local geometry analysis are discussed. The techniques presented in this paper can be used to eliminate errors of milling tool path generation in the area of simultaneous multi-axis NC complex surface machining.

الوصف الرياضي لعدد التفريز وتحديد نصف القطر الفعال للشكل الهندسي للعدة باستخدام مكائن التفريز المتعددة المحاور

### الخلاصة

في هذا البحث تم اشتقاق المعادلات لبناء موديل رياضي يمكن من خلاله وصف الشكل الهندسي للعدة المستخدمة في عملية التفريز المتعددة المحاور. حيث يتم استخدام تقنيات الهندسة التحليلية لفهم شكل حافة القطع الفعالة للعدة المستخدمة، إضافة إلى ذلك فقد تم استخدام ثلاثة أنواع من عدد القطع في الدراسة الحالية. أخيراً، تم تحديد حافة القطع الانية للعدة كذلك تم تحليل عدة القطع في منطقة التماس مع سطح المشغولة. إن البحث الحالي يمكن أن يستعمل لإزالة الأخطاء المتولدة من عمليات التفريز المتعددة المحاور للأسطح المعقدة.

### List of Acronyms and Symbols used in the present research

Symbol	Definition
CC	Shortcut of cutter contact.
CL	Shortcut of cutter location.
CNC	Computer Numerical Control.
ESC	Effective surface curvature
h	The scallop height.
H	The shaft height measured along the cutter axis.
LCS	Local coordinate system
NC	Numerical Control.
$\vec{n}$	The normal direction at the CC point.

\* Production Engineering & Metallurgy Department, University of Technology /Baghdad.

\*\* Engineering College, University of Baghdad / Baghdad.

P	The CC point.
PCS	Program coordinate system
$R$	The cutter radius.
$R_1$	The radial distance of the cutter bottom.
$R_2$	The cutter corner radius.
$R_{y, Eff, X_L=0}$	Effective cutting radius of the cutter on the YL-ZL plane.
$R_{y, Eff, Z_L=0}$	Effective cutting radius of the cutter on the XL-YL plane.
TCS	Tool coordinate system
WCS	Workpiece coordinate system
$a_i$	The angle between the $Z_i$ -axis and the $Z_{i+1}$ -axis measured about the $X_i$ -axis.
$b_1$	The angle from radial line through the cutter tip to the cutter bottom.
$b_2$	The taper angle between the cutter side and the cutter axis.
$r_{y, max}$	The maximum principal curvature of the effective cutting profile.
$r_{y, min}$	The minimum principal curvature of the effective cutting profile.
$y_{Ball}$	The surface geometry of ball cutter.
$y_{Flat}$	The surface geometry of flat cutter.
$y_{Torus}$	The surface geometry of torus cutter.
$\theta$	The angle along the ZT-axis.
$f$	The angle restricted between the axis of the tool and the axis which pass through the cutter contact point which is equal to inclination angle of the plane.
$\lambda$	The lead angle of the cutter relative to the local coordinate system.
$\omega$	The tilt angle of the cutter relative to the local coordinate system.
$\sigma$	The parameter value.

## 1. Introduction

There are seven possible types of cutter for vertical milling applications, cylindrical milling cutter, toroidal milling cutter, ball end milling cutter with cylindrical shank, ball end milling cutter without shank, barrel milling cutter, conical milling cutter, and ball end milling cutter with conical shank. The generalized cutter geometry can be described by several parameters as shown in Fig.(1). [1]. In order to define

a cutter correctly, the above parameters must fulfill the following constrains:

$$R_1 \geq 0, R_2 \geq 0, 0^\circ \leq b_1 < 90^\circ, \\ -90^\circ < b_2 < 90^\circ$$

Note that  $b_2$  is positive when sloping is outward, negative when sloping is inward from the cutter side.

As shown in Fig.(2), based on the generalized cutter geometry, three

common used cutters can be easily defined as follows

(a) Torus or Toriadal (Fillet-end)cutter:

$$R_1 + R_2 = R, \quad b_1 = 0^\circ, \quad \text{and} \\ b_2 = 0^\circ$$

(b) Cylindrical (Flat-end) cutter:

$$R_1 = R, \quad R_2 = 0, \quad b_1 = 0^\circ, \quad \text{and} \\ b_2 = 0^\circ$$

(c) Ball-end cutter:  $R_1 = 0$ ,  $R_2 = R$ ,  $b_1 = 0^\circ$  and  $b_2 = 0^\circ$ .

## 2. Coordinate Definition:

Before deriving the mathematical equation to describe the end mill cutter, the coordinate system must be established. Four orthogonal coordinate systems are defined to assist the calculation; These are: **Tool coordinate system** (TCS,  $X_T$ - $Y_T$ - $Z_T$ ), **local coordinate system** (LCS,  $X_L$ - $Y_L$ - $Z_L$ ), **workpiece coordinate system** (WCS,  $X_W$ - $Y_W$ - $Z_W$ ), and **program coordinate system** (PCS,  $X_P$ - $Y_P$ - $Z_P$ ), and it is necessary for the analysis of the milling control to describe the outer surface of the cutter.

The TCS is used to describe the outer surface of a generalized cutter. As shown in Fig.(3), the  $X_T$ -axis is defined along the cutting direction, and the  $Y_T$ -axis is defined along the tool axis. The  $Z_T$ -axis is defined by the cross product of the  $X_T$ -axis and the  $Y_T$ -axis. The origin is located at the tip of the cutter.

A LCS is used to analyze the cutting operation at the CC point. As shown in Fig.(4), the  $X_L$ -axis is always lying in the current cutting direction, and the  $Y_L$ -axis is in the surface normal direction. The  $Z_L$ -axis is determined by

the cross product of the  $Y_L$ -axis and  $X_L$ -axis. In multi-axis machining, the cutter is first rotated by a lead angle ( $\lambda$ ) about the  $Z_L$ -axis, and then a tilt angle ( $\omega$ ) about the  $Y_L$ -axis. In general, the angles have the following constrains:  $0^\circ \leq \lambda < 90^\circ$ , and  $0^\circ \leq \omega \leq 90^\circ$ .

WCS and PCS can be chosen arbitrarily by the user. As shown in Fig.(5), WCS is taken as the reference coordinate system of the workpiece, and therefore all the workpiece geometrical data can be determined. In the generation of CC points and CL data, the positions of points and the corresponding tool orientations are generated relative to WCS. Also, as shown in Fig.(5), PCS is taken as the reference coordinate system of the machine controllers, and therefore all the NC codes data can be imported. For the convenience of the calculation, the origin of PCS is recommended to be located at the intersection of two rotational axes, and its three axes are defined along three translation axes of the NC machine, respectively.

## 3. Mathematical description of end mill cutters:

The mathematical basis for controlling milling is a description of the outer surface of the cutting tool on an orthogonal tool coordinate ( $X_T$ - $Y_T$ - $Z_T$ ) basis, this basis is then moved along the sculptured surface to be milled. In the following, the analytical description of various tool surfaces in terms of a moving tool coordinate basis ( $X_T$ - $Y_T$ - $Z_T$ ) is introduced.

**Ball cutter:** a ball-end mill cutter is considered. As shown in Fig (6), a tool

coordinate basis ( $X_T - Y_T - Z_T$ ) is defined on the cutter. The  $X_T$  -axis is defined along the cutting direction and  $Y_T$  -axis is defined along the tool axis. The  $Z_T$  -axis is defined by the  $X_T$  - and  $Y_T$  -axis, using the right-hand rule. The boundary of a ball-end mill cutter consists of two essential shapes (a quarter circle and a straight line). The surface of a ball-end mill cutter can be described by  $\Psi_{Ball}$  as:

$$\Psi_{Ball}(q, f, b)_T = \begin{pmatrix} R_2 \sin q \sin f \\ R_2(1 - \cos f) + bH \\ R_2 \cos q \sin f \end{pmatrix}_T \dots(1)$$

( $\Psi_{Ball}$ ) Represents the surface geometry of ball cutter, ( $f$ ) The angle restricted between the axis of the tool and the axis which passes through the cutter contact point (the angle at the corner of the cutter portion), ( $H$ ) is the length of the tool shaft, ( $R_2$ ) is the cutter radius, ( $q$ ) is the angle from the  $Z_T$  -axis and  $0^\circ \leq q \leq 360^\circ$ , as shown in Fig.(6). To understand the surface geometry of the ball cutter from equation (1) the magnitude of the parameters ( $b, f$ ) must be utilized as follows:

- When  $b = 0^\circ$  and  $0^\circ \leq f \leq 90^\circ$ , equation (1) represent the quarter circle of the ball-end mill.
- When  $f = p/2$  and  $b \in [0,1]$ , equation (1) describe the shaft of the ball-end mill.

Using equation (1), it is important to take care that ( $f$ ) and ( $b$ ) are never allowed to vary simultaneously over their respective parameter intervals. Either  $b = 0^\circ$  is fixed, in this case  $\Psi_{Ball}$  describes the bottom portion of a ball-end cutter  $q$  and  $f$  vary, or  $f = p/2$  is fixed, in this case  $\Psi_{Ball}$  in equation (1) describes a cylindrical surface when  $q$  and  $b$  vary.

**Flat cutter:** Fig.(7) shows a flat-end mill cutter and the tool coordinate basis. The surface of a flat-end mill cutter can

$$\Psi_{Flat}(q, a, b)_T = \begin{pmatrix} aR_1 \sin q \\ bH \\ aR_1 \cos q \end{pmatrix}_T \dots (2)$$

be described by  $\Psi_{Flat}$  as:

( $\Psi_{Flat}$ ) Represents the surface geometry of flat cutter, ( $a$ ) The angle between  $Z_T$ -axis and  $Z_{i+1}$ -axis measured about  $X_i$ -axis. Also ( $H$ ) is the length of the tool shaft, ( $R_1$ ) is the cutter radius, ( $q$ ) is the angle from the  $Z_T$  -axis and  $0^\circ \leq q \leq 360^\circ$ , as shown in Fig.(7). To understand the surface geometry of the flat cutter from equation (2) the magnitude of the parameters ( $b, a$ ) must be utilized as follows:

- When  $b = 0^\circ$  and  $a \in [0,1]$ , equation (2) describe the bottom of the flat-end mill cutter.
- When  $a = 1$  and  $b \in [0,1]$ , equation (2) describe the shaft of the flat-end mill cutter.

**Torus cutter:** Fig.(8a,b) shows a torus-end mill cutter, the surface of a torus-shaped cutter can be described as  $\Psi_{Torus}$  as follows:

$$\Psi_{Torus}(q, f, a, b)_T = \begin{pmatrix} (aR_1 + R_2 \sin f) \sin q \\ R_2(1 - \cos f) + bH \\ (aR_1 + R_2 \sin f) \cos q \end{pmatrix}_T \dots (3)$$

( $\mathcal{Y}_{Torus}$ ) Represents the surface geometry of torus cutter. From Fig.(8a,b) it can be found that torus cutter is described by the combination of ball and flat end mill cutters, the surface geometry of the torus cutter can be described depending on the surface geometry of the ball and flat end mill cutters, since ( $f$ ) describes the corner portion and  $0^\circ \leq f \leq 90^\circ$ , and ( $q$ ) is the angle from the  $Z_T$ -axis and  $0^\circ \leq q \leq 360^\circ$ . In equation (3), ( $a$ ) describes the bottom portion of the cutter and ( $b$ ) describes the portion of the shaft. Using equation (3), care must be taken that  $f$ ,  $a$  and  $b$  are never allowed to vary simultaneously over their respective parameter intervals. However, the points on different portions of  $\Psi_{Torus}$  can be described by a different combination of parameters. Using equation (3), the bottom portion of the cutter can be described by  $\{a \in [0,1], f = 0^\circ, b = 0^\circ\}$  which means surface geometry of flat cutter, the torus portion by  $\{a = 0, 0^\circ \leq f \leq 90^\circ, b = 0^\circ\}$  which means surface geometry of ball cutter, finally the shaft portion can be described at

$\{a = 1.0, f = p/2, b \in [0,1]\}$ . Actually, equation (3) is a generalized representation for all three different end mills. Both the descriptions  $\Psi_{Ball}$  and  $\Psi_{Flat}$  in equations (1) and (2) are the special cases of the description  $\Psi_{Torus}$  in equation (3). If the variables  $R_2$  and  $f$  of  $\Psi_{Torus}$  in equation (3) are set to be  $R_2 = 0$  and  $f = 0^\circ$ , then the formula reduces to  $\Psi_{Flat}$  of a flat-end mill cutter as described in equation (2). On the other hand, if the  $R_1$  and  $a$  of  $\Psi_{Torus}$  in equation (3) are set to be  $R_1 = 0$  and  $a = 0$ , the formula reduces to  $\Psi_{Ball}$  of a ball-end mill as described in equation (1). Starting from here,  $y(q, f, a, b)_T^G$  (in tool coordinate basis) is used to represent the generalized tool description of the different end mills which can either be  $\Psi_{Torus}$ ,  $\Psi_{Flat}$  or  $\Psi_{Ball}$ .

**4. Kinematics motion of inclined cutters on multi axis CNC machine:**

In multi axis machining, besides the three translation axis of a NC machine, the cutter can be rotated about one or two translation axis of the NC machine. As shown in Fig.(9), this basis is then moved along the sculptured surface to be milled. For 5-axis machining, the tools have two degrees of freedom in rotation about two of the three translation axes. Besides the inclination angle  $I_L$  about the  $Z_L$ -axis, the tools are allowed to rotate about the  $Y_L$ -axis

with a tilt angle  $w_L$ . The general tool formula  $y(q, f, a, b, I_L, w_L)_L^G$  for describing an inclined tool in 5-axis machining can be derived by multiplying the tool formula in equation (3) with the rotation matrix describing a rotation  $I_L$  about the Z<sub>L</sub>-axis, another rotation of  $w_L$  about the Y<sub>L</sub>-axis, and a translation matrix from the tool coordinate basis (X<sub>T</sub> - Y<sub>T</sub> -Z<sub>T</sub>) to the local coordinate basis (X<sub>L</sub> - Y<sub>L</sub> -Z<sub>L</sub>). The kinematics tool motion can be derived as follows:[2,3]

$$\Psi(q, f, a, b, I_L, w_L)_L^G = Rot(-w_L).Rot(-I_L).$$

$$Tran \begin{pmatrix} -R_1 - R_2 \sin I_L \\ -R_2(1 - \cos I_L) \\ 0 \end{pmatrix} + \Psi(q, f, a, b)_T^G$$

$$= \begin{pmatrix} \cos w_L & 0 & -\sin w_L \\ 0 & 1 & 0 \\ \sin w_L & 0 & \cos w_L \end{pmatrix} \begin{pmatrix} \cos I_L & \sin I_L & 0 \\ -\sin I_L & \cos I_L & 0 \\ 0 & 0 & 1 \end{pmatrix} \times$$

$$\begin{pmatrix} (aR_1 + R_2 \sin f) \sin q - R_1 - R_2 \sin I_L \\ R_2(1 - \cos f) + bH - R_2(1 - \cos I_L) \\ (aR_1 + R_2 \sin f) \cos q \end{pmatrix}_T$$

.... (4)

The function  $y(q, f, a, b, I_L, w_L)_L^G$  in equation (4) is a generalized tool description of a cutter oriented with orientation  $(I_L, w_L)$  in the local coordinate basis (X<sub>L</sub>-Y<sub>L</sub>-Z<sub>L</sub>) for 5-axis machining. For 4-axis machining, the tool formula  $y(q, f, a, b, I_L)_{L,4axis}^G$  is actually a special case of the generalized tool description  $y(q, f, a, b, I_L, w_L)_L^G$  in equation (4) by

setting  $(w_L = 0^\circ)$ . Depending on the selection of the parameters  $q, f, a$  and  $b$ , all the surface points of the tool oriented with  $(I_L, w_L)$  in 4-and 5-axis machining can be described by the generalized tool formula  $y(q, f, a, b, I_L, w_L)_L^G$  in equation (4).

**5. Effective radius of tool surface geometry:**

In sculptured surface machining, there are two major machined surface errors: gouging and undercut [4]. As shown in Fig.(10), if the cutter overcuts into the part surface with negative error during machining and the error is larger than the required surface tolerance, it is called gouging. In addition, materials are left on the part surface after machining. These excess materials (positive error) left on the part surface after machining are called undercuts or cusps. If the cusps left are larger than allowable tolerance, these cusps need to be removed by other processes such as grinding or polishing, which are time-consuming and expensive operations. The cutter gouges into the part surface as surface point P1 with a negative error of d between P1 and P2. In the meantime, there is an undercut (positive) error Δ below the cutter which causes material to be left on the surface after machining. As shown in Fig. (10), an undercut error occurs between surface point P4 and point P3 on the cutter.

To reduce the cusp height left on the machined surface in multi-axis machining, the instantaneous cutting profile should get as close as possible to

the local part surface. To avoid gouging, the effective cutting radius  $R_{y, Eff}$  of the cutting profile should be no greater than the radius ( $k$ ) of the local surface curvature ( $k = [1 / R]$ ). Fig. (11) shows that the local curvature  $r$  on the instantaneous cutting plane ( $Y_L$ - $Z_L$  plane) can be calculated by the following equation: [5]

$$r_{x_L=0} = r_{min} \cos^2 s + r_{max} \sin^2 s$$

where  $s = \cos^{-1}(\vec{X}_p \cdot \vec{X}_L)$

....(5)

An explanation is needed for finding  $R_{y, Eff}$  of the torus-end mill cutter first, because this type of cutter includes the property of two other cutters (ball and flat) in shape. Then  $R_{y, Eff}$  for the ball and flat end mill cutter is found depending on equation (4) as follows:

The two principal curvatures  $r_{y, max}$  and  $r_{y, min}$  of the torus corner of the filleted cutter can be found by inclining the cutter with a non-zero  $I_L$  angle (and  $w_L = 0^\circ$ ) as shown in Fig. (12). The maximum curvature of the corner portion of a filleted cutter is equivalent to the inverse of the radius of the corner torus, as shown in Fig.(12). The maximal curvature  $r_{y, max}$  can be represented as: [5]

$$r_{y, max} = \frac{1}{R_2}$$

....(6)

To find the minimum principal curvature  $r_{y, min}$  orthogonal to the

maximum principal curvature, the tool surface description  $y(q, f, I_L, w_L)_L^G$  of the torus shaped cutter is used, and this means that the curvature of the instantaneous cutting profile must be found when the tool is inclined forward with an inclination angle  $I_L$  (and  $w_L = 0$ ). Also this means that the minimum curvature  $r_{y, min}$  can be found by setting the tilting angle  $w_L = 0$  and  $f = I_L$  at the cutter contact point, as shown in Fig. (12 a). For the cutter contact point,  $q$  is equivalent to  $p / 2$  according to the definition of the tool coordinate basis. From equation (4), the following function  $H(q, I_L, w_L = 0)_L^G$  can be found for the instantaneous cutting profile after inclining the cutter with a given angle  $I_L$  and setting  $w_L = 0$ ,  $a = 1$ ,  $b = 0$ , and  $f = I_L$ :

$$H(q, I_L, w_L = 0)_L^G = \Psi(q, f = I_L, a = 1, b = 0, I_L, w_L = 0)_L^G$$

$$= \begin{pmatrix} \cos I_L & \sin I_L & 0 \\ -\sin I_L & \cos I_L & 0 \\ 0 & 0 & 1 \end{pmatrix} \times \begin{pmatrix} (R_1 + R_2 \sin I_L) \sin q - R_1 - R_2 \sin I_L \\ R_2(1 - \cos I_L) - R_2(1 - \cos I_L) \\ (R_1 + R_2 \sin I_L) \cos q \end{pmatrix}_T$$

$$= \begin{pmatrix} \cos I_L (R_1 + R_2 \sin I_L) (\sin q - 1) \\ \sin I_L (R_1 + R_2 \sin I_L) (1 - \sin q) \\ (R_1 + R_2 \sin I_L) \cos q \end{pmatrix}_L$$

....(7)

The curvature at a point on the profile  $H(q, I_L, w_L = 0)_L^G$  can be found by using equation (8) as follows:[6].

$$r(q, I_L, w_L)_H = \left[ \left[ \left( \frac{\partial H(q, I_L, w_L)}{\partial q} \right) \cdot \left( \frac{\partial^2 H(q, I_L, w_L)}{\partial q^2} \right) \right] \times \left[ \left( \frac{\partial H(q, I_L, w_L)}{\partial q} \right) \cdot \left( \frac{\partial^2 H(q, I_L, w_L)}{\partial q^2} \right) \right] \right]^{1/2} \left[ \left( \frac{\partial H(q, I_L, w_L)}{\partial q} \right) \cdot \left( \frac{\partial H(q, I_L, w_L)}{\partial q} \right) \right]^3 \dots (8)$$

Consequence, by substitute both the first and second order derivations of  $H(q, I_L, w_L = 0)_L^G$  from equation (7) into equation (8) the curvature of the instantaneous cutting profile can be found as follows:

$$r(q, I_L, w_L = 0)_H = \frac{\sin I_L}{(R_1 + R_2 \sin I_L) \sqrt{(\sin^2 q + \sin I_L \cos^2 q)^3}} \dots (9 a)$$

Since the angle  $q$  is equivalent to  $p/2$  at the cutter contact point, the minimum curvature  $r_{y, \min}$  of point CC can be found by substituting  $q = p/2$  into equation (9 a) as:

$$r_{\Psi, \min} = r \left( q = \frac{p}{2}, I_L, w_L = 0 \right)_{H, CC^*} = \frac{\sin I_L}{(R_1 + R_2 \sin I_L)} \dots (9 b)$$

On the torus portion of the tool surface, the principal directions of the maximal and minimal curvatures occur when  $w_L$

= 0, as shown in Fig.(12). In 5-axis machining, a tool is oriented with an orientation  $(I_L, w_L)$ . The angle between the instantaneous cutting direction ( $X_L$  -axis) and the principal direction ( $Xp$ -axis) is equivalent to  $w_L$  angle ( $S = w_L$ ), as shown in Fig.(11). Substituting equations (9b) and (6) into  $H(q, I_L, w_L = 0)_L^G$  can be found, which is on the  $Y_L$ - $Z_L$  plane normal to equation (5), the curvature of the instantaneous cutting profile the current cutting direction  $X_L$ -axis with an arbitrary tool orientation  $(I_L, w_L)$ , also using equation (5), the curvature  $r(I_L, w_L)_{y, X_L=0}$  on the  $Y_L$ - $Z_L$  plane that is normal to cutting direction  $X_L$  can be calculated, and the effective cutting radius  $R_{y, Eff, X_L=0}$  of the torus shaped cutter on the  $Y_L$ - $Z_L$  plane can then be derived as follows:

$$R(I_L, w_L)_{\Psi, Eff, X_L=0} = [r(I_L, w_L)_{\Psi, X_L=0}]^{-1} = [r_{\min} \cos^2 w_L + r_{\max} \sin^2 w_L]^{-1} = \left[ \left( \frac{\sin I_L}{R_1 + R_2 \sin I_L} \right) \cos^2 w_L + \left( \frac{1}{R_2} \right) \sin^2 w_L \right]^{-1} = \frac{R_2 (R_1 + R_2 \sin I_L)}{R_2 \sin I_L \cos^2 w_L + (R_1 + R_2 \sin I_L) \sin^2 w_L} \dots (10)$$

On the other hand, the curvature  $r(I_L, w_L)_{y, Z_L=0}$  of a torus-shaped cutter on the  $X_L$ - $Y_L$  plane can be found by using equation (5) and setting  $(S = w_L + p/2)$  as follow:

$$\begin{aligned}
 r_{Z_L=0} &= r_{\min} \cdot \cos^2 S + r_{\max} \cdot \sin^2 S \\
 &= r_{\min} \cdot \cos^2(w_L + p/2) + r_{\max} \cdot \sin^2(w_L + p/2) \\
 &= r_{\min} \cdot [\cos(w_L) \cdot \cos(p/2) - \sin(w_L) \cdot \sin(p/2)] \\
 &\quad \cdot [\cos(w_L) \cdot \cos(p/2) - \sin(w_L) \cdot \sin(p/2)] \\
 &\quad + r_{\max} \cdot [\sin(w_L) \cdot \cos(p/2) + \sin(p/2) \cdot \cos(w)] \cdot \\
 &\quad [\sin(w_L) \cdot \cos(p/2) + \sin(p/2) \cdot \cos(w)] \\
 &= r_{\min} \cdot \sin^2 w + r_{\max} \cdot \cos^2 w \\
 &= r_{\min} \cdot \sin^2 S + r_{\max} \cdot \cos^2 S
 \end{aligned}$$

...(11)

So, the effective cutting radius  $R_{y, Eff, Z_L=0}$  of a torus-shaped cutter on the  $X_L$ - $Y_L$  plane can then be found as follows:

$$\begin{aligned}
 R(I_L, w_L)_{\Psi, Eff, Z_L=0} &= [r(I_L, w_L)_{\Psi, Z_L=0}]^{-1} \\
 &= \left[ \left( \frac{\sin I_L}{R_1 + R_2 \sin I_L} \right) \sin^2 w_L + \left( \frac{1}{R_2} \right) \cos^2 w_L \right]^{-1}
 \end{aligned}$$

...(12)

By using equations (10) and (12), the effective cutting radii  $R_{y, Eff, X_L=0}$  and  $R_{y, Eff, Z_L=0}$  of a torus-shaped milling cutter can be found with an arbitrary tool orientation  $(I_L, w_L)$  for 5-axis sculptured surface machining.

For a case of  $w_L = 0$  and  $I_L = p/2$ , the  $R_{y, Eff, X_L=0}$  becomes  $(R_1 + R_2)$  which is equivalent to the shaft radius. If  $w_L = 0$  and  $I_L = 0$ , the  $R_{y, Eff, X_L=0}$  becomes  $(\infty)$  which reflects the flat bottom of the torus-shaped cutter.

For the case of the tilt angle  $w_L = 0$ , equations (10) and (12) become the following:

$$\begin{aligned}
 R(I_L, w_L = 0)_{y, Eff, X_L=0} &= \frac{(R_1 + R_2 \sin I_L)}{\sin I_L} \\
 &= \frac{1}{r_{\min}} \Rightarrow r_{\min} = \frac{\sin I_L}{(R_1 + R_2 \sin I_L)}
 \end{aligned}$$

....(13)

$$\begin{aligned}
 R(I_L, w_L = 0)_{y, Eff, Z_L=0} &= R_2 = \frac{1}{r_{\max}} \\
 \Rightarrow r_{\max} &= \frac{1}{R_2}
 \end{aligned}$$

.....(14)

**Ball-end cutter:**  $R_1 = 0$ ,  $R_2 = R$  so the effective cutting radius  $R_{y, Eff, X_L=0}$  of the ball shaped cutter on the  $Y_L$ - $Z_L$  plane can be written as follows, depend on equation (10):

$$\begin{aligned}
 R(I_L, w_L)_{\Psi, Eff, X_L=0} &= \frac{R_2 (R_1 + R_2 \sin I_L)}{R_2 \sin I_L \cos^2 w_L + (R_1 + R_2 \sin I_L) \sin^2 w_L} \\
 &= \frac{R_2^2 \sin I_L}{R_2 \sin I_L \cos^2 w_L + R_2 \sin I_L \sin^2 w_L}
 \end{aligned}$$

.....(15 a)

For  $(w = 0)$ :

$$\begin{aligned}
 R(I_L, w_L)_{\Psi, Eff, X_L=0} &= \frac{R_2 \sin I_L}{\sin I_L} \\
 &= R_2 = \frac{1}{r_{\min}}
 \end{aligned}$$

..... (15 b)

On the other hand the effective cutting radius  $R_{y, Eff, Z_L=0}$  of a ball-shaped cutter on the  $X_L$ - $Y_L$  plane can then be written as follows:

$$R(I_L, w_L)_{\Psi, Eff, Z_L=0} = \frac{R_2(R_1 + R_2 \sin I_L)}{R_2 \sin I_L \sin^2 w_L + (R_1 + R_2 \sin I_L) \cos^2 w_L} = \frac{R_2^2 \sin I_L}{R_2 \sin I_L \sin^2 w_L + R_2 \sin I_L \cos^2 w_L} \dots(16 a)$$

For( $w = 0$ ):

$$R(I_L, w_L)_{\Psi, Eff, Z_L=0} = \frac{R_2 \sin I_L}{\sin I_L} = R_2 = \frac{1}{r_{max}} \dots(16 b)$$

**Flat-end cutter:** the equations (10),(12) are true when the curvatures of the corresponding surface are continuous. Therefore, these equations are suitable for a torus-end cutter and a ball-end cutter, but are not suitable for a flat-end cutter which has infinite curvature at the torus portion. So for a flat-end cutter, the effective cutter radius at the CC point in the  $\hat{X}$  direction can be calculated using equation (17) as follows:[7].

$$R_1 = R, R_2 = 0$$

$$R(I_L, w_L = 0)_{y, Eff, X_L=0} = R(I_L, w_L)_{\Psi, Eff, Z_L=0} = \frac{\sin I_L}{R_1 \cdot \cos^2(a - (w - P/2))} \dots(17)$$

$a$  : The angle between the  $Z_i$ -axis and the  $Z_{i+1}$ -axis measured about the  $X_i$ -axis. The equations (13), (14), (15 a,b), (16 a,b) and (17) are general solution for torus, ball and flat cutters and it can be used in 3-axis machining and also in multi-axis machining, also it must be noticed that in three axis machining the angle ( $w$ ) is equal to zero and the angle ( $I$ ) means the angle between tool axis and the surface normal to the workpiece in each point at CC point. Whereas, in multi axis machining the magnitude of ( $w, I$ ) depends on the number of translation motions and rotation motions.

**6. Results:**

This research presents the calculation of the cutter radius, as follows:

- Derivation of equations that describing mathematically three types of cutters used in the present work.
- Describe the kinematics motion of inclined cutters on multi axis CNC machine using transmtion matrix.
- Derive the equations to get the effective cutter radius of the tool surface geometry.

Finally, from these above procedures the selection of suitable cutter for milling operation in 3 and multi-axis

machine can be made depending on the reducing values of errors on machining surface.

### 7. Conclusions:

From the present research and the derived equations, it was noticed that the cutter radius is not responsible for making machining on the plane of the workpiece, but there is an effective cutter radius which is responsible for this machining. Each cutter has an effective radius and this radius is change according to the shape of cutter and to the curvature of workpiece, also to the number of axes that the milling machine can be moved (three or multi-axis machine), and the effective cutter radius can be calculated depending on equations (13, 14) for tours cutter, equations (15, 16) for ball cutter and equation (17) for flat cutter.

### References:

- [1] G. Yu, "General tool correction for five-axis milling", *Journal of Advanced Manufacturing Technology*, vol.10, pp.374-378, 1995.
- [2] Johnj.Craig, "Introduction to robotics mechanics and control", Second edition, 1989.
- [3] Y.-S. LEE, "Mathematical modelling using different end mills and tool placement problems for 4- and 5-axis NC complex surface machining", *Journal of prod. res.*, vol.36, pp.785-814,1998.
- [4] Chih-Ching Lo, "A tool-path control scheme for five-axis machine tools", *Journal of Machine Tools & Manufacture*, vol.42, pp.79-88, 2002.
- [5] Y. S. Lee, Ji, H, "Surface interrogation and machining strip

evaluation for 5-axis CNC die and mold machining", *Journal of Production Research*, vol.35, pp. 225-252, 1997.

[6] Barnhill,R. E, T. Lyche and L. L. Schumaker, "Geometry processing: curvature analysis and surface-surface intersection", In *Mathematical Methods in Computer Aided Geometric Design*, New York, Academic Press, pp. 51- 60, 1989.

[7] M.Z.He, Huang, "Five-axis machining improvement via cutting error control and tool orientation smoothing", Taiwan university, 2006.

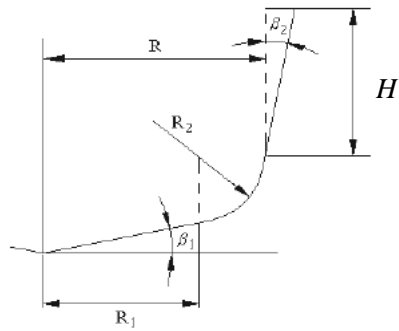


Figure (1) The definitions of a generalized cutter,[1]

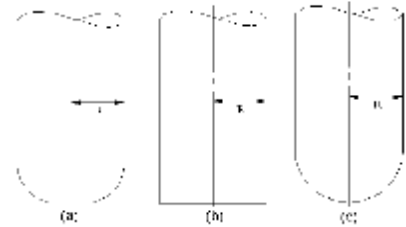


Figure (2) Different types of the end milling cutters

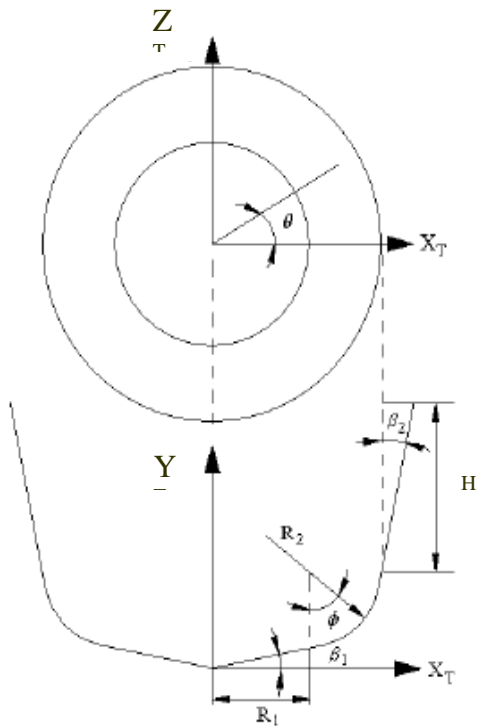


Figure (3) The definition of tool coordinate system (TCS)

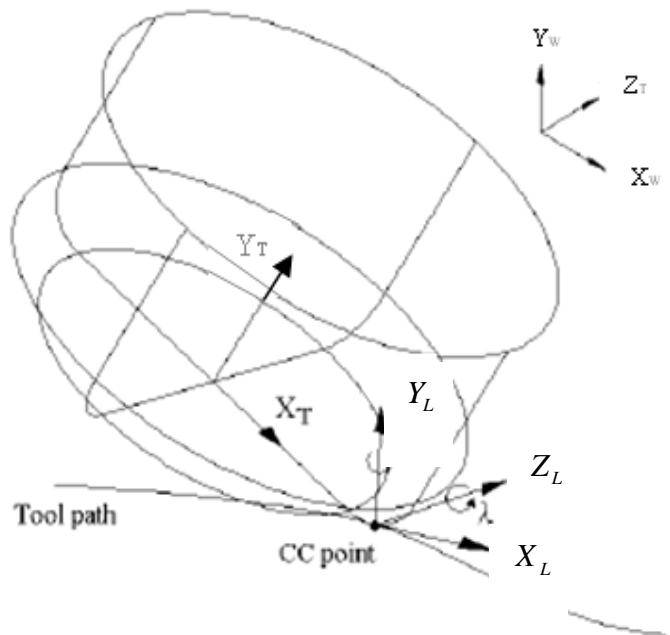


Figure (4) The definition of local coordinate system (LCS)

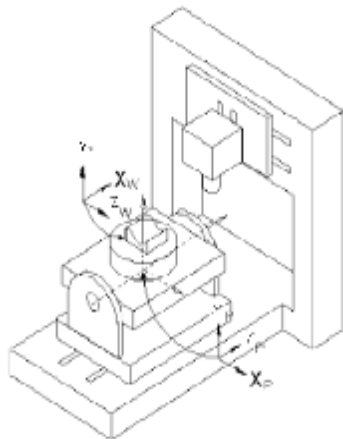


Figure (5) The definition of workpiece coordinate system (WCS ) and program coordinate system (PCS)

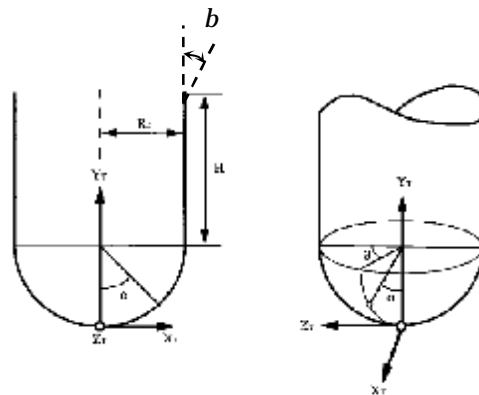


Fig (6) Ball-end mill cutter in the tool coordinate basis (XT-YT-ZT).

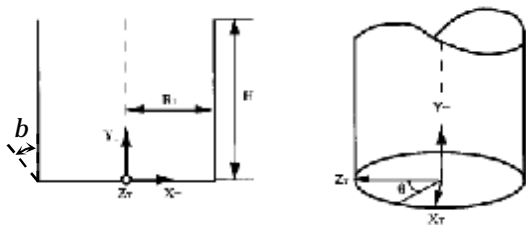


Figure (7) Flat-end mill cutter in the tool coordinate basis (Xr-Yr-Zr)

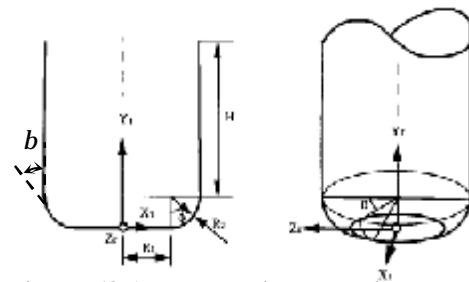


Figure (8a) Torus mill cutter in the tool coordinate basis (XT-YT-ZT)

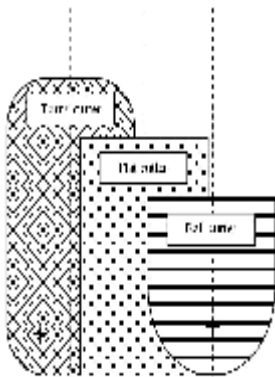


Figure (8 b) Torus mill cutter results from the collection of ball and flat end mill cutters

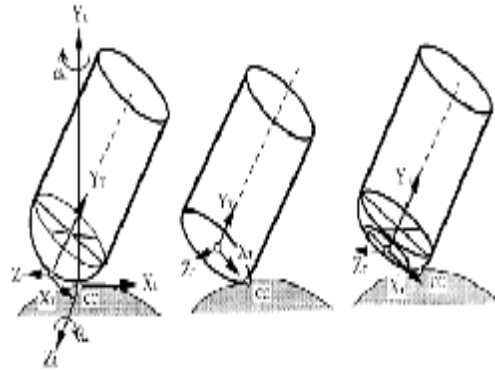
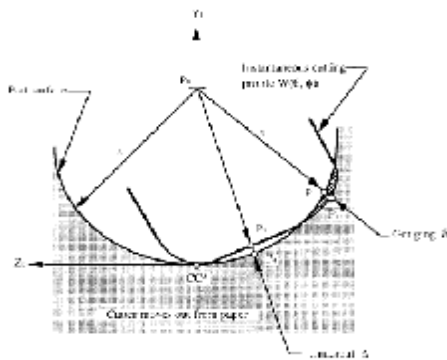


Figure (9) Tools rotated with both the inclination angle  $I_L$  and the tilt angle  $W_L$ , [3]



Figure(10). Show gouging and undercut error. [4]

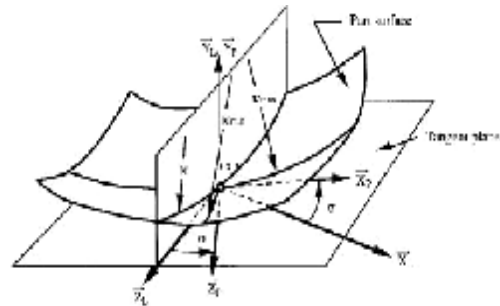
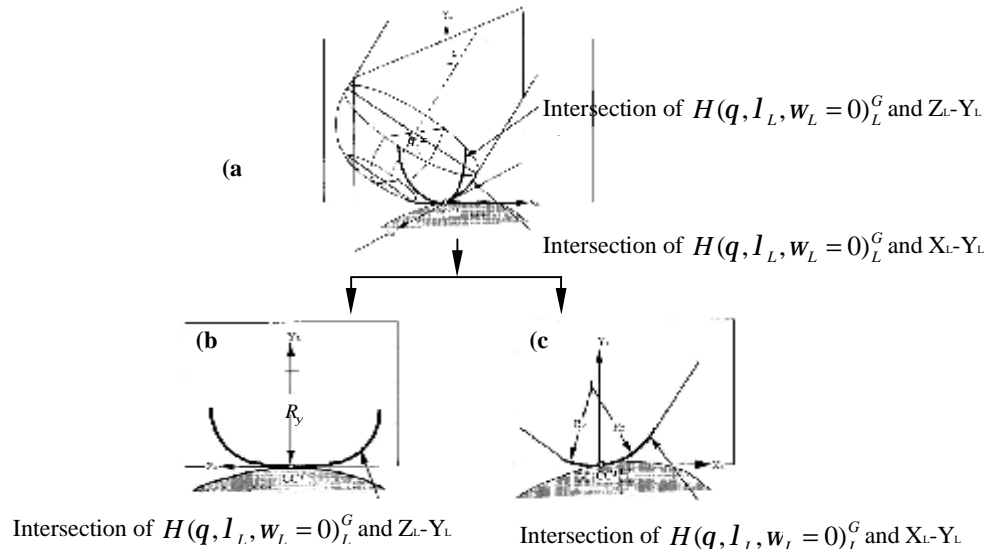


Figure (11) Local surface curvature ( $k$ ) on the  $Y_L - Z_L$  plane normal to cutting direction ( $X_L$ ), [5]



**Figure (12) Describes minimum and maximum curvatures at CC point on the torus corner.**